Study on current conduction mechanism in evaporated Cu_2S thin films

M. RAMYA[*], S. GANESAN[a]

Department of Physics, Sri Shakthi Institute of Engg. & Tech., Coimbatore 641 062, Tamil Nadu, India
[a]*Department of Physics, Government, College of Technology, Coimbatore 641 013, Tamil Nadu, India*

Cu_2S being an II-VI compound has attracted much attention in opto-electronic device applications. Cu_2S were synthesized by vacuum evaporation under a pressure of 10^{-6} torr at an evaporation rate of 3Å /sec. Rotary drive is employed to obtain uniformity in film thickness. Thicknesses of the film were measured by using quartz crystal monitor. Resistivity of Cu_2S thin films were measured by four probe method. The electrical properties of Al- Cu_2S -Al (MSM) structures were studied using current-voltage characteristics. The conductivity was found to exhibit two distinct mechanisms within the applied fields. The possible conduction mechanism prevailing in Cu_2S thin films were also discussed. High thickness Cu_2S thin film exhibit high conductivity whereas conductivity decreases towards the lower thickness. Band gap has been calculated for different thicknesses and is found that band gap decreases with increase in film thickness.

1. Introduction

The principal advantages of II-VI compounds for terrestrial solar photovoltaics are low cost and ease of deposition of good quality films from these materials by a variety of growth methods. Films grown from each of these compounds exhibit several crystalline forms and variety of orientation with respect to substrate depending on deposition parameters. Due to their high photosensitivity, high absorption co-efficient and direct band gap these II-VI semiconductors are of great interest in electronic and opto- electronic devices.

Copper Sulphide being an II-VI compound is an important material from the point of basic research, because it is known to exist in several crystallographic and stoichiometric forms. Copper Sulphide is found to exist in two forms at room temperature as 'Copper-rich' and 'Copper-poor'. Copper rich phases exist as chalcocite, djurlite, digenite and anilite. Copper poor phase are existing as co-vellite. It is well established that Cu_2S is the optimum proportion for obtaining high efficiency solar cells with high stability against oxidation and degradation. The Cu_2S is P-type conductivity, which is due to the presence of copper vacancies, which acts as electron acceptors and gives rise to free holes. Cu_xS (x=1- 2) thin films have numerous technological applications such as sensors [1], as thermo electric converters, high capacity cathode materials in lithium batteries [2], non-linear optic materials [3], nano-meter scale switches [4], as solar radiation absorber [5] and in micro-electromechanical-system (MEMS) devices. In recent years there has been much interest in Copper Sulphide films because of its use as an absorber in CdS/Cu_2S thin film solar cells, which still hold promise for large scale terrestrial photovoltaic power generation. Cu_2S is known to be excellent heterojunction partner with CdS. Much attention has been focused on thin film CdS/Cu_2S heterojunction due to their great promise as low cost solar power converter owing to their high efficiency with improved stability.

Cu_2S thin films have been prepared by various techniques such as Reactive Sputtering, Spray Pyrolysis [6], Modified Chemical Method [7], photochemical method [8] and Vacuum Evaporation method [9]. Vacuum evaporation method has been successful in depositing high purity films with high quality. There is lack of definite result concerning the temperature dependence of conductivity for Cu_2S thin films, which needs further investigation. The purpose of the present work was therefore to report the conduction mechanism in Cu_2S thin film prepared by vacuum evaporation.

2. Experimental details

2.1 Film preparation

Vacuum evaporation is simple and most widely used technique for synthesizing high purity semiconductor films. Cu_2S thin films of different thickness were deposited on properly cleaned glass substrate with the help of Hind High Vacuum coating unit at the vacuum, 10^{-6} torr. Pure (99.99%) copper sulphide powder was used as the source material. Prior to deposition of thin films, high purity aluminium electrode was vacuum evaporated on properly cleaned glass substrate on which the films were deposited. Molybdenum boats were used as source heater and the glass substrate was mounted on the holder with heating arrangement. The thicknesses of the film were measured by quartz crystal monitor whereas temperature was measured with the help of fine wire chromel and alumel thermocouple. The substrate to source distance was

optimized to be at 18.1 cm inside the vacuum chamber. Rotary drive is employed to maintain uniformity in film thickness. Constant rate of evaporation 3Å/sec was maintained throughout the sample preparation. Electrical resistivity measurements were carried out on the as prepared Cu$_2$S samples.

2.2 Film characterization

The most commonly used technique for measuring resistivity is the four point probe method. The arrangement consists of PID controlled oven (model-PID-200 scientific equipment and services, Roorkee, India) in combination with low current source (model-LCS-01) and digital micro voltmeter (model-DMV-001). It consists of four collinear metal probes with sharpened tips, which are placed on the flattened surface of the material to be measured. Constant current I is passed through the outer two probes and the potential difference is measured across the inner two probes. The nominal value of the probe spacing is equal to the distance of 2 mm between the adjacent probes. The potential difference is measured using a high input impedance voltmeter.

Current-Voltage characteristics of the MSM structure were studied by employing digital micro ammeter in series with the capacitor and the voltage source. All the studies were performed under the vacuum of about 680 mm Hg. The Current - Voltage behavior were studied in the temperature range 300-400 K and the temperature during measurements was maintained using variable voltage transformer. A copper constantan thermocouple is used for the temperature measurements. A potential of 20 volts was applied using DC regulated power supply in series with the digital voltmeter.

Photo current was measured by taking silver paste as a contact electrode at 1 cm separation applied on the film surface. The samples are kept in the measurement chamber. A halogen lamp was used for white light and the intensity of light was measured in mW/cm^2 by placing a surya-amp at the position of the sample. The photocurrent was measure using micro ammeter.

Capacitance –Voltage measurements were made at room temperature using LCR, meter (LCR 819,GW Instek. Good will company instrument Ltd., Taiwan). The capacitance dependence of bias was studied by applying reverse bias (0-2V) for frequencies in the range 30 KHz to 100 KHz. For this purpose the internal bias of the LCR meter is switched OFF and the external bias in switched ON.

2.3 Theory and calculation

The electrical properties of the film are greatly influenced by the deposition conditions and nature of the substrate. Resistance is related to film thickness and free path of the charge carriers. The resistivity of the film is very sensitive to deposition conditions and nature of the material. According to the modern quantum electronic theory, electrical conduction in metals is due to electrons, while electrical resistivity results from the scattering of

electrons by the lattice. Therefore resistivity is the measure of metal lattice displacement from prefect regularity [10]. The electrical resistance in metals may arise from variety of causes, such as temperature, dissolved impurities and vacancies. Resistivity of the films were calculated using the formula

$$\rho = \rho_0 \exp (Eg/KT) \qquad (1)$$

Where 'ρ' is resistivity, 'ρ$_0$' is constant, 'K' is the Boltzmann constant, 'T' is the absolute temperature and 'Eg' is the activation energy.

Different types of conduction mechanism takes place in semiconductor films namely tunneling, impurity conduction, space charge limited conduction, Schottky emission and Poole Frenkel conduction. Information about the conduction mechanism prevailing in the Cu$_2$S thin film is obtained from the Current- Voltage characteristics of Cu$_2$S thin films. The conduction mechanism in these are mainly governed by the grain boundary defect states. In the low field region the conduction mechanism will be ohmic whereas in the high electric field the mechanism will be non-ohmic. The samples subjected to high field usually show a linear relation between log I and E$^{1/2}$ Where 'I' is the current, 'E' is the applied electric field. These linear behavior indicates that conduction is controlled either by poole-frenkel or schottky mechanism. In the schottky mechanism electrons are transported by thermionic emission across metal-semiconductor interface, whereas in the poole-frenkel effect electrons are thermally emitted from traps to conduction band as a result of lowering of columbic potential barrier by an external field, thereby increasing the probability of electron [11]. Current- voltage relation according to poole-frenkel or schottky has the form

$$I = I_0 \exp \left(\frac{\beta E^{1/2} - V_g}{KT} \right) \qquad (2)$$

Where 'E' is the electric field, 'β' is the field lowering co-efficient, V$_g$ is the trap depth level below the bottom of conduction band in the case of poole-frenkel or work function difference in the case of schottky effect. The constant β is given by

$$\beta = \left(\frac{e^2}{\alpha \pi \varepsilon_0 \varepsilon_r} \right) \qquad (3)$$

Where 'e' is the charge of the electron, 'ε$_r$' is the relative dielectric constant, 'ε$_o$' is the permittivity of free space and 'α' is constant equal to 1 or 4 for poole-frenkel or schottky effect respectively. When the applied field increases the potential barrier decreases on the right side of the trap, thereby making it easier for the electron to move form trap to conduction band. As a result the barrier height is reduced due to applied electric field [12]. The activation energy has been determined using the relation

$$I = I_0 \exp \left(\frac{-E}{KT} \right) \qquad (4)$$

The donor density, flat band potential and barrier height can be determined form the change in capacitance as a function of applied potential using the inverse of Mott - Schottky relation [13,14]. The donor density (N_D) can be calculated form the known equation

$$\frac{1}{s} = \frac{2}{q\xi_0\xi A^2} \, cm^{-3} \qquad (5)$$

where 'S' is the slope , 'A' is the area of the electrode, 'q' is the electronic charge, 'ξ_0' the permittivity of free space, 'ξ' the dielectric constant of the material.

The number of states can be calculated from the measured capacitance at low and high frequencies using the relation

$$N_{IS} = (C_{LF} - C_{HF})/q \qquad (6)$$

Where N_{IS} is the total number of interfaces states, C_{LF} and C_{HF} are the capacitance at lower and higher frequencies respectively, 'q' is the electronic charge.

Barrier height (ϕ_B) are calculated using the relation

$$(\phi_B) = \frac{\varsigma}{KT} \, \ln\left(\frac{AA^*T^2}{I_S}\right) \qquad (7)$$

where the parameters have their usual meaning.

When the film is illuminated by light, additional photo excited carriers are generated in the films, as a result, part of thermally excited carrier together with large number of photo-generated carriers neutralizes some fraction of localized charges in the depletion regions in the grain boundary potential barriers. Photoconductivity signal versus intensity of incident light is described by the relation

$$I_{pc} \, \alpha \quad (I_L)^\alpha \qquad (8)$$

where 'I_{pc}' is photo current, 'I_L' is the incident photon flux and 'α' is the empirical constant.

3. Results and discussion

Fig. 1 and 2 shows the XRD pattern of Cu_2S thin film of 1000 Å and 7000 Å thickness respectively. Fig. 1 reveals the XRD spectra of lower thickness film with very weak peaks (mixed state of amorphous and polycrystalline nature) whereas the presence of prominent peaks (at 2θ = 46.3, 27.7) in Fig. 2 shows the polycrystalline nature of the film, indicating the corresponding phase transformation in the film.
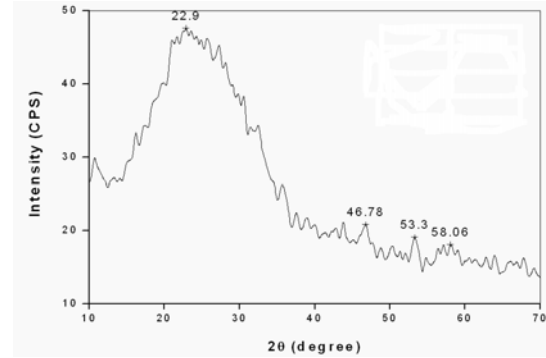

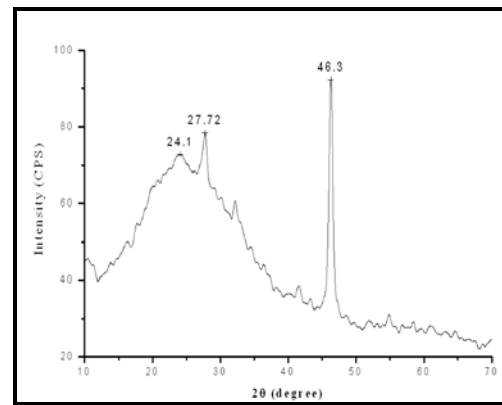Fig. 1. XRD pattern of Cu_2S thin films of 1000 Å thickness.

Fig. 2. XRD pattern of Cu_2S thin films of 7000 Å thickness.

Fig. 3 represents the variation of resistivity with inverse of absolute temperature for various currents (30-90 µA) of 1000 Å thickness. It was observed that resistivity initially decreases with temperature and attains a minimum value called as transition temperature and further increases with temperature. The critical temperature is estimated within (383-403 K). These observations show that the material behaves as semi conducting nature at lower temperature and metallic above critical temperature [7,16].
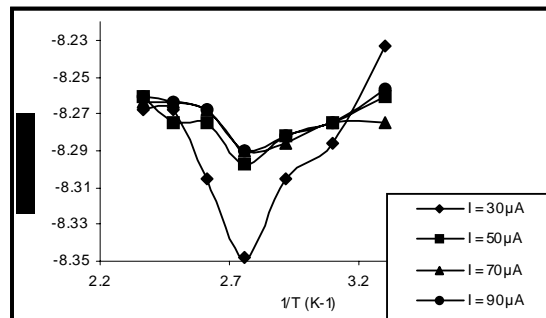

Fig. 3. Variation of resistivity with Inverse of temperature for Cu_2S film of 1000 Å thickness.

Constant temperature was applied across the Cu_2S sample and the variation of resistivity with different thickness was studied at constant current (Fig. 4). The resistivity was found to increase in the lower thickness range (up to 5600Å) and further decreases for higher thickness, and the decrease in resistivity is due to phase transformation that exist in the film [17,18] which agrees with structural properties of Cu_2S thin film reported in this paper. Further the decrease in resistivity of the film at higher thickness reveals that the film has high conductivity at higher thickness.
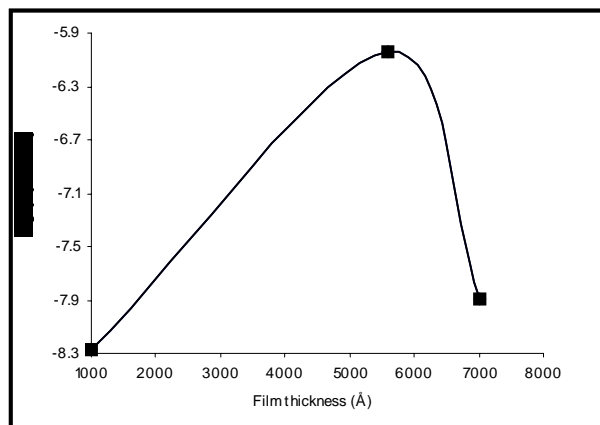

Fig. 4. Variation of log resistivity with film thickness.

Fig. 5 shows the current versus voltage characteristics of Cu_2S thin films of 1000 Å thickness at different temperatures. The current voltage characteristics have two distinct regions, low voltage region and high voltage region. At low voltage region the curve exhibit linear dependence of current on voltage whereas at high voltage region the curve exhibit high power law, ie ($I \propto V^n$). For lower bias the injected charge carrier is lower than the thermally generated carrier density, where n is equal to unity and that leads to ohmic behavior [19,20,21,22]. Ohmic behavior exist as long as free carrier density continues to be in thermal equilibrium, when the carrier density becomes greater than the thermal equilibrium the situation changes and this occurs at higher bias level where n is less than 2 [23]. These observations do not support the possibility for Space Charge Limited Conduction and hence it may be inferred that the conduction mechanism in these films may be either Schottky or Poole-Frenkel. In order to investigate the conduction mechanism prevailing in the Cu_2S thin film, the samples are subjected to high electric field between Log I and $E^{1/2}$. Fig. 6 shows the variation of log current with the square root of the applied field for Cu_2S thin film

of 1000 Å thickness. The values of field lowering coefficient (β_{exp}) were calculated from the figure and are compared with the theoretical value of (β_{theory}). Table 1 shows the calculated Poole-Frenkel co-efficient value of 1000 Å thickness and the value have been found in the range 1.07×10^{-5} (m V)$^{1/2}$ to 1.99×10^{-5} (mV)$^{1/2}$ in the temperature 303 K - 403 K. Evidently the experimental value of 'β' is found to lie very near to theoretical value of Poole-Frenkel co-efficient (β_{pf}). Thus the conduction mechanism in Cu_2S thin film is most probably be the Poole-Frenkel effect based on the results obtained. It is observed that the curve exhibit linear current field characteristics at higher temperatures and within the ambient temperature range (323 K - 343 K) the Poole-Frenkel co-efficient decreases as the ambient temperature increases. Further a graph plotted between log (J/T^2) and 1/T for different voltages showed a straight line which again confirms the poole-frenkel effect in Cu_2S thin film.
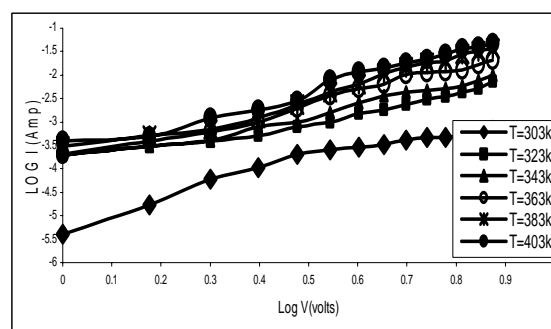

Fig. 5. Variation of current with Voltage measured at different temperature For Cu_2S film of 1000 Å thickness.
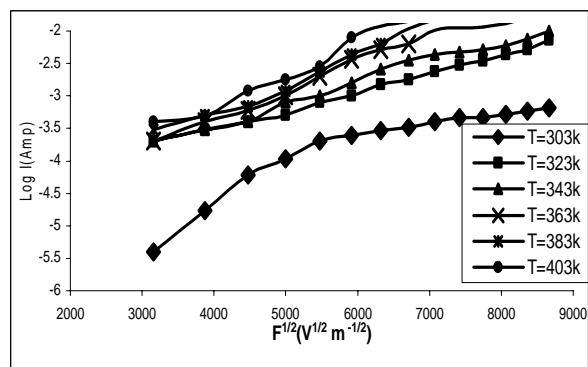

Fig. 6. Variation of current with square root of applied field measured at different temperature for Cu_2S film of 1000 Å thickness.

Table 1. Experimental and theoretical values of (β) for Cu₂S film.

Temperature (K)	Experimental field lowering coefficient (β) $10^{-5}(mV)^{1/2}$	Theoretical field lowering coefficient (β) $10^{-5}(mV)^{1/2}$	
		Poole Frenkel (a=1)	Richardson Schottky (a=4)
303	1.07	1.51	0.75
323	1.78		
343	1.35		
363	1.79		
403	1.99		

Slope values for different voltages of Cu₂S thin film are calculated from the plot of log current versus inverse of absolute temperature and the band gap are calculated using the slope value in (5).The calculated values are found to be in the range (0.2 ----0.09) eV for Cu₂S thin film. From the Table 3 it is evident that the activation energy decreases with increase in applied voltage, indicating that the potential barrier has been lowered in the presence of applied field [24]. Moreover, the band gap is reduced with increase in film thickness which is due to increase in grain size of the film. This increase in grain size effectively reduces inter grain boundary defect states and thereby reduces band gap [25]. The intercept at V=0 yields the zero activation energy. The estimated zero activation energy for film of different thickness is shown in Table 2.

Table 2. Variation of band gap with applied voltage.

Voltage (volts)	Activation Energy (eV) for different thicknesses	
	1000 Å	7000 Å
2	0.197	0.148
4	0.118	0.112
6	0.112	0.098
ΔE_0	0.30	0.15

The variations of photo current with applied voltage for different illuminations are shown in Fig. 8. The conductivity is found to increase exponentially with applied voltage as well as intensity [26, 27] which imply that Cu₂S thin film is free from trap. The estimated maximum photocurrent was found to be 5(μA). Moreover, the photocurrent increases with increase in film thickness which again confirms the decrease in band gap of the material.
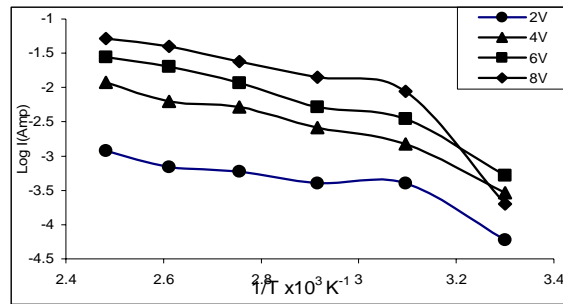

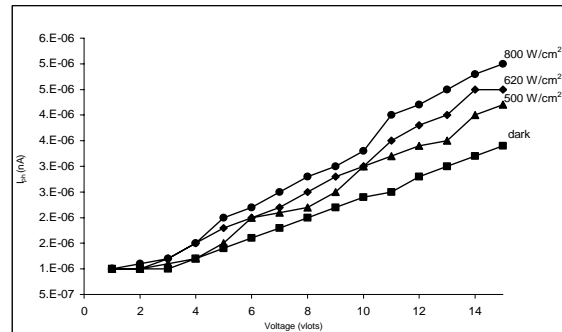*Fig. 7. Variation of Current with inverse of temperature for different Voltages for Cu₂S film of 1000 Å thickness.*

Fig. 8. Variation of photo Current (I ph) with Voltage measured at different illumination for Cu₂S film of 5600 Å thickness.

Fig. 10 shows the frequency dispersion of capacitance of Cu₂S films in dark at two different voltages. From the plots it was observed that at low frequency the capacitance shows larger value and the decreasing behavior of capacitance with increasing frequency suggests a contribution of the junction space charge from relatively slow deep level states at or near the interface [28]. Moreover at higher frequencies the frequency dispersion of capacitance was almost constant. The total number of interface states (N_{IS}) was calculated at low (70 kHz) and high (100 kHz) frequencies using the equation (6) and was found to be 1.8×10^{17} for 1000Å thickness. The ionized

donor density (N$_D$) was calculated from the Mott – Schottky plot (slope of $1/C^2$ Vs bias voltage) at V$_B$ close to zero and using the slope value in (5), is found to be $5.57 \times 10^{16}/cm^3$. A negative voltage shifts in the frequency indicates the presence of positive charge carriers in the film [29]. The extrapolated value of voltage at $1/C^2=0$ gives the value of flat band potential as 2.4V for 1000 Å thickness [24]. The barrier heights (ϕ_B) are calculated using (7) and are entered in Table 3 along with ionized donor density (N$_D$), number of interface states(N$_{IS}$) and flat band potential(V$_b$) for Cu$_2$S thin film of 1000Å thickness. The calculated value shows that higher thickness films have low barrier height, which again confirms phase transformation [30]. Hence it is concluded that higher thickness Cu$_2$S films with low resistivity and low barrier height has superior conducting behavior than low thickness Cu$_2$S films.
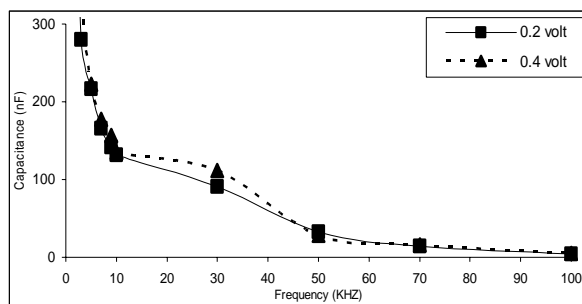

Fig. 9. Frequency dispersion of capacitance in dark for Cu$_2$S film of 5600 Å thickness measured at different voltages.
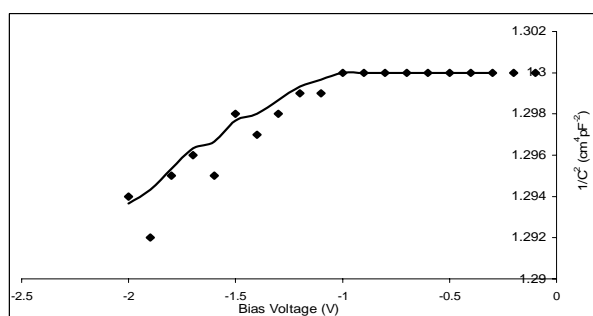

Fig. 10. Variation of capacitance with voltage for Cu$_2$S film of 1000 Å thickness measured at constant frequency.

Table 3. Electrical parameters of Cu$_2$S thin film.

Parameters	Al-Cu$_2$S-Al device
Ionized donor density (N$_D$)	$5.57 \times 10^{16}/cm^3$
Number of interface states(N$_{IS}$)	1.8×10^{17}
Diffusion potential(V$_b$)	2.4 V
Barrier Height(ϕ_B)	0.300 eV

4. Conclusions

The conduction mechanism in evaporated Cu$_2$S thin films was analyzed from the current-voltage characteristics. Structural properties of the film clearly indicate that the films coated at higher thickness shows slight deviation from stoichiometry. Resistivity studies revealed that low temperature Cu$_2$S thin films exhibit high conductance while high temperature film has high resistance. Resistivity initially increases with increase in film thickness and then decreases for films of higher thickness. The possible conduction mechanism in Cu$_2$S films is found to be Poole-Frenkel type. The ionized donor density, Flat band potential, barrier height are calculated form the capacitance voltage measurements. Moreover higher thickness Cu$_2$S thin films bear good conducting nature than lower thickness films.

References

[1] Abhay A. Sagade, Ramphal Sharma, Sensors and Actuators B: Chemical, **133,** 135 (2008).
[2] J. S. Chung, H. J. Sohn, J. Power Sources, **108**, 226 (2002).
[3] Titipun Thongtem, Anukorn Phuruangrat and Somchai Thongtem, Materials letters, **64**, 136 (2010).
[4] Sakamoto, T. Sunamura, H. Kawaura, H Applied Physics Letters, **82**, 3032 (2003).
[5] Yong Caizhang, Tao Qiao, Xiao Ya Hu, Journal of Crystal Growth, **268**, 64 (2004).
[6] S. Y. Wang, W. Wang, Z. H. Lu, Mater. Sci. Eng., B **103,** 184 (2003).
[7] H. M. Pathan, J. D. Desai, C. D. Lokhande, Appl. Surf. Sci., **202,** 47 (2002).
[8] Jiban Podder, Ryohei Kobayashi, Masaya Ichimura Thin Solid Films, **472,** 71 (2005).
[9] M. Ramya, S. Ganesan, Iranian Journal of Material Science and Engineering, 8, **34** (2011)
[10] L. I. Maissel, R. Glang, Hand book of Thin Film Technology, Mc Graw Hill Book Company, New York (1970).
[11] M. M. El-Samanoudy, Applied Surface Science, **207**, 219 (2003).
[12] W. R. Harrell, J. Frey, Thin Solid Films, **352**, 195 (1999).
[13] N. F. Mott, Proc. R. Soc.,London, **171**, 27 (1939).
[14] W. Schottky, Z. Phys., **118**, 539 (1942).
[15] Nourhene Kamoun Allouche,Tarak Ben Nasr, Cathy Guasch and Najoua Kamoun Turki, C. R. Chimie, **13**, 1364 (2010).
[16] C. D. Lokhande, H. M. Pathan, M. Giersig, H. Tributsch, Appl. Surf. Sci., **187,** 201 (2002).
[17] S. Duchemin, I. Youm, J. Bougnot, M. Cadene Solar Energy Materials, **15**, 337 (1987).
[18] M. Ramya, S. Ganesan, International Journal of Pure and Applied Physics, **3**, 243 (2010).
[19] N. Mazumdar, R. Sarma, B. K. Sarma, H. L. Das, Bull. Mater.Sci, **29**, 11 (2006).
[20] R. D. Gould, B. B. Ismail, Vacuum, **50**, 99 (1998).
[21] Svetlana Erokhina, Victor Erokin, Claudio Nicolini,

Colloids and Surfaces, **645**, 198 (2002).
[22] Youngseok Lim, Young-Woo Ok, Sung-Ju Tark, Yoonmook Kang, Donghwan Kim ,Current Applied Physics, **9**, 890 (2009).
[23] Saeed Salem Babkir, Azhar Ahmad Ansari, Najat Mohamed Al-Twarqi, Materials Chemistry and Physics, **127**, 296 (2011).
[24] R. Sathyamoorthy, C. Sharmila, P. Sudhagar, C. Chandramohan, S. Velumani, Materials Characterization, **58**, 730 (2007).
[25] K. R. Pradip Kali ta, B. K. Sarma, H. L. Das, Bull. Mater, Sci., **26,** 613 (2003).

[26] W. D. Gill, R. H. Rube, Journal of Applied Physics, **41**, 3731 (1970).
[27] K. R. Pradip Kali ta, B. K. Sarma, H. L. Das, Bull. Mater., Sci., **26,** 613 (2003).
[28] S. Senthilarasu, R. Sathyamoorthy, S. Lailtha, A. Subbarayan, Solid State Electronics, **49**, 813 (2005).
[29] S. S. Nandi, S. Chaterjee, S. S. Samanta, G. K. Dalpati, P. K. Bose, S. Varma, Shivprasad Patil, C. K. Maiti Bull. Mater. Sci., **26**, 365 (2003).
[30] Abhay A-Sagade, Ramphal Sharma, Sensors and Acutators B **133**, 135 (2008).

*Corresponding author: ramsthangam@gmail.com